Published in final edited form as:
Biomacromolecules. 2012 May 14; 13(5): 1663–1674. doi:10.1021/bm300381d.

Optimal Poly(L-lysine) Grafting Density in Hydrogels for Promoting Neural Progenitor Cell Functions

Lei Cai[†], **Jie Lu**[§], **Volney Sheen**[§], and **Shanfeng Wang**[†,‡,*]

[†]Department of Materials Science and Engineering, The University of Tennessee, Knoxville, TN 37996

[‡]Biosciences Division, Oak Ridge National Laboratory, Oak Ridge, TN 37831

[§]Department of Neurology, Beth Israel Deaconess Medical Center, Harvard Medical School, Boston, MA 02115

Abstract

Recently we have developed a photo-polymerizable poly(L-lysine) (PLL) that can be covalently incorporated into poly(ethylene glycol) diacrylate (PEGDA) hydrogels to improve their bioactivity by providing positive charges. To explore the potential of these PLL-grafted PEGDA hydrogels as a cell delivery vehicle and luminal filler in nerve guidance conduits for peripheral and central nerve regeneration, we varied the amount of pendent PLL chains in the hydrogels by photo-crosslinking PEGDA with weight compositions of PLL (ϕ_{PLL}) of 0, 1%, 2%, 3%, and 5%. We further investigated the effect of PLL grafting density on E14 mouse neural progenitor cell (NPC) behavior including cell viability, attachment, proliferation, differentiation, and gene expression. The amount of actually grafted PLL and charge densities were characterized, showing a proportional increase with the feed composition ϕ_{PLL}. NPC viability in 3D hydrogels was significantly improved in a PLL grafting density-dependent manner at days 7 and 14 post-encapsulation. Similarly, NPC attachment and proliferation were promoted on the PLL-grafted hydrogels with increasing ϕ_{PLL} up to 2%. More intriguingly, NPC lineage commitment was dramatically altered by the amount of grafted PLL chains in the hydrogels. NPC differentiation demonstrated a parabolic or non-monotonic dependence on ϕ_{PLL}, resulting in cells mostly differentiated toward mature neurons with extensive neurite formation and astrocytes rather than oligodendrocytes on the PLL-grafted hydrogels with ϕ_{PLL} of 2%, whereas the neutral hydrogels and PLL-grafted hydrogels with higher ϕ_{PLL} of 5% support NPC differentiation less. Gene expression of lineage markers further illustrated this trend, indicating that PLL-grafted hydrogels with an optimal ϕ_{PLL} of 2% could be a promising cell carrier that promoted NPC functions for treatment of nerve injuries.

Keywords

Hydrogels; Poly(L-lysine) (PLL); Poly(ethylene glycol) diacrylate (PEGDA); Neural progenitor cells; Grafting density

Introduction

Peripheral nerve injury and spinal cord injury (SCI) caused by trauma or chronic neurodegenerative diseases such as amyotrophic lateral sclerosis or even multiple sclerosis are complicated clinical problems that affect millions of people.[1-3] Although some success

*To whom correspondence should be addressed. swang16@utk.edu. Tel: 1-865-974-7809; Fax: 1-865-974-4115.

has been achieved for short peripheral nerve gaps using autologous or artificial nerve grafts from biodegradable polymers, bridging large injury gaps is still challenging.[1,2] Much effort has been focused on developing numerous tissue engineering approaches for SCI, while current clinical treatments still offer little hope for successful functional recovery.[3] Neural stem/progenitor cells with the ability to self-renew and differentiate into neuronal and glial lineages have shown great promise in these two scenarios.[1,4] They are able to remyelinate axons and secrete neurotrophic factors, which can stimulate axonal regeneration, if transplanted to the site of injury *in vivo*.[1,4] Therefore, it is crucial to develop biodegradable cell delivery vehicles with bioactivity that can foster cell survival and guide desired differentiation for achieving functional reconnection and recovery of the injured nerves.[1-6]

Polyethylene glycol (PEG) is a widely used polymer for biomedical applications because of its characteristics including good biocompatibility, non-immunogenicity, resistance to protein adsorption, and tunable mechanical properties.[6,7] Previously we have synthesized photo-crosslinkable PEG diacrylate (PEGDA) via facile condensation by reacting the two hydroxyl end groups with acryloyl chloride using potassium carbonate (K_2CO_3) as a proton scavenger.[8,9] Because of its inert nature to cellular affinity, numerous soluble factors as well as functional groups such as acrylated Arg-Gly-Asp (RGD) ligands and cationic 2-(methacryloyloxy)-ethyl-trimethylammonium chloride (MTAC) have been incorporated into PEG-based hydrogel to improve its bioactivity.[10-15] PEGDA hydrogels conjugated with RGD ligands, a cell-binding peptide, could significantly improve attachment, spreading, and mineralization of osteoblasts and osteogenesis of mesenchymal stem cells (MSCs) in a dosage-dependent manner, meaning that a higher concentration resulted in better cell responses before saturation.[11-13] Cationic MTAC covalently bonded hydrogels generally exhibited an optimal charge density to best promote cell behavior such as endothelial cell attachment and dorsal root ganglion (DRG) neurite extension.[14,15] As an alternative approach, we recently developed a photo-polymerizable poly(L-lysine) (PLL) with positive charges and used it to modify PEGDA hydrogels for promoting nerve cell functions.[8] PLL is known to modulate cell adhesion via a non-receptor-mediated cell binding mechanism via electrostatic bond formation between positive charges on PLL and the negatively charged cell membrane.[16] At a lower charge density than MTAC, PLL-grafted hydrogels could better promote attachment, proliferation, and differentiation of pheochromocytoma (PC12) cells and neural progenitor cells (NPCs).[8]

Our PLL-grafted hydrogels serve as an ideal system to achieve better fundamental understanding of the role of PLL chains in regulating cell behavior. They have a well-defined structure and ease of measuring dissociated positive charge density and PLL grafting density. In contrast, standard PLL-coated substrates have several disadvantages, including the lack of long-term stability and constant density, influence on cell behavior by soluble or desorbed PLL, and difficulty in determining the positive charge density on these substrates.[16,17] For copolymers of PLL-*g*-PEG synthesized through the functionalization of the amino groups of PLL, fewer free amine groups but more secondary amine groups can lead to loss of positive charges and the extent varies with molar ratios of PLL/PEG, although it is believed that high free amine concentrations can be cytotoxic.[18,19] That said, our prior work on PLL-grafted hydrogels raises several fundamental questions about hydrogel and NPC function. It is unclear how the grafting density of PLL influences hydrogel and NPC properties. Moreover, the dose dependency of grafted PLL in the hydrogels in regulating NPC differentiation into all three central nervous system (CNS) lineages (neurons, astrocytes and oligodendrocytes) has not been explored.

Here we have performed a systematic study of PEGDA hydrogels grafted with different amounts of PLL to investigate the effect of PLL grafting density on E14 mouse NPC behavior in terms of viability in encapsulation, attachment, proliferation, differentiation, and

gene expression. The hydrogel networks were prepared using the PEGDA with a nominal molecular weight of 10000 g/mol, which was previously found to best support NPC attachment, proliferation, and differentiation compared with other two stiffer hydrogels made from PEGDAs with nominal molecular weights of 3000 and 1000 g/mol.[8] We photo-crosslinked PLL with this PEGDA and varied the weight compositions of PLL (ϕ_{PLL}) from 0-5%. The actual amount of PLL grafted on the hydrogels and their charge densities have been characterized using energy dispersive x-ray spectroscopy (EDS) and zeta-potential measurements. The coverage of PLL chains on the hydrogels was estimated and compared with the feeding ϕ_{PLL}. NPC viability in encapsulation in the hydrogels, and attachment and proliferation on the hydrogels were analyzed in a serum-free growth media. Using immunohistochemistry and real-time polymerase chain reaction (PCR), the ratios of NPC differentiated toward all three lineages were quantified and correlated with their morphology and gene expression. By demonstrating PLL grafting density-dependent NPC responses, we have not only achieved better understanding on the effect of grafted PLL, but also offered a versatile PLL-grafted PEGDA hydrogel with an optimal ϕ_{PLL} as a cell delivery vehicle to promote NPC functions for nerve regeneration.

Experimental Section

Synthesis and Photo-crosslinking

All chemicals were purchased from Sigma-Aldrich (Milwaukee, WI) unless otherwise noted. PEGDA (M_n = 14500 g/mol, M_w = 15300 g/mol) was synthesized by reacting PEG with acryloyl chloride in the presence of K_2CO_3.[8] Photo-polymerizable PLL (M_n = 3060 g/mol, M_w = 3750 g/mol) was synthesized via ring-opening polymerization of *Z*-L-Lys-*N*-carboxyanhydride using allylamine as an initiator.[8] 4-(2-hydroxyethoxy)phenyl-(2-hydroxy-2-propyl)ketone (Irgacure 2959, Ciba Specialty Chemicals, Tarrytown, NY) was used as a photo-initiator for crosslinking. The precursor solutions were prepared by dissolving 0, 1, 2, 3, and 5 wt.% photo-polymerizable PLL in deionized (DI) water with 30 wt.% PEGDA and 0.05 wt.% Irgacure 2959. The precursor solution was transferred into a mold formed by a Teflon spacer (0.37 mm, thickness) between two glass plates and then exposed for 10 min to UV light (λ = 365 nm) generated from a high-intensity (4800 μw/cm^2) long-wave UV lamp (SB-100P, Spectroline). The distance between the sample and the lamp head was ~7 cm. Except for measuring swelling ratios and gel fractions, the hydrogels were fully soaked and washed in DI water for 1 day and repeated three times to remove sol fraction before physical characterization and cell studies.

Hydrogel Characterization

To examine the swelling ratios and gel fractions, three hydrogels from each group were dried immediately after crosslinking and weighed (W_0). Then the hydrogels were immersed in DI water or cell culture media for 1 day, blotted dry, and weighed (W_d). The swollen hydrogels were completely dried in vacuum and weighed again (W_s). The swelling ratios and gel fractions were calculated using the equations of (W_s - W_d)/W_d and $W_d/W_0 \times 100\%$, respectively.[20-23] Linear viscoelastic properties of neutral and PLL-grafted PEGDA hydrogels, including storage modulus G', loss modulus G'', and viscosity η as functions of frequency, were measured on a strain-controlled rheometer (RDS-2, Rheometric Scientific) with a small strain (γ = 1%) in the frequency (ω) range of 0.1-100 rad/s.[20-23] A 25 mm diameter parallel plate flow cell and a gap of ~1.0 mm were used, depending on the thickness of the hydrogel. To measure the zeta-potential values of the hydrogels, the samples were homogenized into particles (~1 μm, diameter) in 4-(2-hydroxyethyl) piperazine-1-ethanesulfonicacid sodium salt (HEPES) buffer solution (HEPES 0.005 M, $NaHCO_3$ 0.0155 M, NaCl 0.14 M, pH = 7.4).[24] Zeta-potential measurements were then performed on a Delsa™ Nano C Zeta Potential Analyzer (Beckman Coulter, Brea, CA). EDS (S-3500,

Hitachi Instruments, Tokyo, Japan) was used to determine the weight fractions of C, O, and N in the total amount of these three atoms on the completely dried PLL-grafted PEGDA hydrogel surfaces at an accelerating voltage of 20 kV. The amount of grafted PLL was then calculated from the weight percentage of N atoms.

Viability of Photo-encapsulated NPCs

NPCs from E14 mouse cortex were cultured in tissue culture flasks in an incubator with 5% CO_2 and 95% relative humidity at 37 °C using serum-free growth media containing DMEM/F12 medium (Invitrogen, Carlsbad, CA) with 2% StemPro neural supplement (Invitrogen), 20 ng/mL basic fibroblastic growth factor (bFGF, Invitrogen), 20 ng/mL recombinant human epidermal growth factor (EGF, Invitrogen), 1% GlutaMAX (Invitrogen), and 1% penicillin/streptomycin (Invitrogen). Cell culture media was changed every two days and cells were split when they were 70% confluent. NPCs were trypsinized, centrifuged, and re-suspended at a density of ~200000 cells/mL in the precursor solution and crosslinked under UV light for 10 min. The cell-laden hydrogels were then immersed in the cell culture media and cultured for 7 and 14 days. Cell viability was determined using LIVE/DEAD Viability/Cytotoxicity kit (Invitrogen) at each time point. Separate images were taken for viable cells with green fluorescence and non-viable cells with red fluorescence. Cell viability or the percentage of green cells was calculated from the number of green cells divided by the total number of cells. At least 500 cells were counted for each hydrogel group. Foe each hydrogel, four disks were used and evaluated in all the cell studies.

NPC Attachment and Proliferation

Prior to cell studies, neutral and PLL-grafted PEGDA hydrogels were cut into disks (~8 × ~1.0 mm, diameter × thickness), sterilized in 70% alcohol solution overnight, and rinsed adequately in phosphate-buffered saline (PBS). NPCs were seeded onto the sterile hydrogel disks in a 48-well tissue culture polystyrene (TCPS) plate at a density of ~15000 cells/cm^2 for 12 h, 1, 4, and 7 days. Cells were also seeded on empty wells at the same density as the positive control. The attached cells at each time point were trypsinized and the cell number was determined using a hemacytometer. Attached cells were also fixed in 4% paraformaldehyde (PFA) solution at room temperature for 10 min and rinsed with PBS. Cell nuclei were stained with 4',6-diamidino-2-phenylindole (DAPI) at room temperature for photographing using an Axiovert 25 light microscope and an AxioCam ICm1 camera (Carl Zeiss, Germany). The cell number identified by DAPI-stained cell nuclei was counted from at least seven fluorescence images and averaged. For immunostaining, fixed cells were blocked with PBS containing 0.3% Triton X-100 and 1% bovine serum albumin (BSA) at room temperature for 30 min. After blocking, cells were incubated with a diluted primary antibody of mouse monoclonal anti-nestin (1:500) at 37 °C for 1 h and then at 4 °C overnight. After washing using PBS containing 1% BSA three times, cells were stained with a secondary antibody of goat anti-mouse IgG-FITC (1:100) at 37 °C in the dark for 2 h and then washed with PBS three times. Cell nuclei were counter-stained using DAPI. Percentage of nestin positive cells to the total number of cells in each image was counted. At least ten images were analyzed and averaged.

NPC Differentiation

For NPC differentiation, cells were seeded onto the sterile hydrogel disks at a density of ~5000 cells/cm^2. After cells attached, the growth media were removed and replaced with a differentiation media containing DMEM/F12, 1% FBS, 1% GlutaMAX, and 1% penicillin/streptomycin.[31] Cells were cultured in the differentiation media for additional 7 days. Differentiated cells were fixed and blocked using the same procedure mentioned in the previous section. The following primary antibodies were used for immunohistochemistry: mouse monoclonal anti-β-tubulin III (1:500) for immature neurons; rabbit monoclonal anti-

neurofilament 200 (NF, 1:1000) for mature neurons; rabbit monoclonal anti-glial fibrillary acidic protein (GFAP, 1:500) for astrocytes; mouse monoclonal anti-oligodendrocyte marker O4 (1:1000; R&D Systems, Minneapolis, MN) for oligodendrocytes. The secondary antibody of goat anti-mouse IgG-FITC (1:100) was used for staining nestin, β-tubulin III, and O4, while the secondary antibody of CF647 goat anti-rabbit IgG (1:100, Biotium, Hayward, CA) was used for staining NF and GFAP. Differentiation in terms of positive antibody expression was quantified by counting the number of cells that expressed the marker divided by the total number of cells identified by DAPI-stained nuclei. Neurite outgrowth was quantified from images stained with NF. Only neurites longer than the diameter of cell body (~10 μm) were recorded. At least ten images from each group were analyzed and averaged. Based on the total cell number, the number of neurite-bearing cells, the number of neurites per cell, and the length of each neurite, we calculated percentage of cells bearing neurites, the number of neurites per cell or per neurite-bearing cell, average neurite length, and total neurite length per cell or per neurite-bearing cell.

NPC Gene Expression

Differentiated NPCs were trypsinized and total RNA was isolated using RNeasy Mini Kit (Qiagen, Valencia, CA). The amount of total RNA from each sample was quantified using Nanodrop1000 spectrophotometer (Thermo Scientific, Wilmington, DE). Reverse transcription of isolated RNA was then performed using DyNAmo cDNA synthesis kit (Thermo Scientific) according to the manufacturer's protocol. The oligonucleotide primers including nestin, β-tubulin III, neuron specific enolase 2 (NSE), GFAP, myelin oligodendrocyte glycoprotein (MOG), and glyceraldehyde-3-phosphate-dehydrogenase (GAPDH) were used for real-time polymerase chain reaction (PCR) and their sequences are listed in Table 1. Real-time PCR reactions were performed in 25 μL of PCR mixture consisting of each cDNA sample, a specific primer, and a Power SYBR® Green PCR Master Mix (Applied Biosystems, Carlsbad, CA). Thirty PCR cycles with each cycle consisting of denaturation at 94 °C for 30 s, annealing at 55 °C for 30 s, and elongation at 72 °C for 30 s were implemented using a Peltier Thermal Cycler with fluorescence detection systems (PTC-200, MJ Research). The expression of target genes was normalized to the level of GAPDH.

Statistical analysis

All data are presented as mean ± standard deviation. Statistical computations were performed by one-way analysis of variance (ANOVA) followed by Tukey post-hoc test. The values were considered significantly different when the *p*-value was less than 0.05.

Results and Discussion

Hydrogel Characteristics

Using photo-polymerizable and water-soluble PLL with one end group of carbon-carbon double bond, PEGDA hydrogels could be easily and efficiently modified by pendent PLL chains via photo-crosslinking (Figure 1). The bulk and surface properties of PEGDA hydrogels grafted with different amounts of PLL at ϕ_{PLL} of 1-5% were characterized. As shown in Figure 2a, the neutral and PLL-grafted hydrogels had high gel fractions of ~75% at ϕ_{PLL} of 1-3% and ~70% at ϕ_{PLL} of 5%, ensuring integrity and smoothness of the hydrogels after removal of sol fraction. As an indicator of crosslinking density, the swelling ratios in DI water (Figure 2b) were ~15 for the neutral and PLL-grafted hydrogels at ϕ_{PLL} of 1-2% without statistical difference. Because PLL could polymerize by itself at high ϕ_{PLL} and the covalent linkage of PLL along the PEG blocks decreased the crosslinking density, the swelling ratio for hydrogels at higher ϕ_{PLL} of 3% and 5% increased to 16.8 and 19.4, respectively. The swelling ratios in culture media showed the same trend, despite slightly

lower values due to charge screening. The decrease in crosslinking density was commonly seen in many polymer networks heavily grafted with polymer chains bearing one reactive end.[25,26] This phenomenon was also evidenced by rheological properties, where G', G'', and η were proportional to the hydrogel crosslinking density. As shown in Figure 2c, all the neutral and PLL-grafted PEGDA hydrogels demonstrated characteristic curves of hydrogel networks because G' had no frequency dependence in the frequency range of 0.1-100 rad/s and it was constantly greater than G''. Shear thinning behavior in η was found for all the hydrogels (Figure 2d). The shear modulus G, i.e., the average value of G' in the tested frequency range, showed similar values of 9.2 ± 0.3, 9.5 ± 0.3, 8.7 ± 0.2 kPa for the neutral and PLL-grafted hydrogels at ϕ_{PLL} of 1% and 2% and it decreased to 6.7 ± 0.2 and 4.7 ± 0.1 kPa at ϕ_{PLL} of 3% and 5%, respectively.

To precisely quantify the charge densities of the PLL-grafted hydrogels and the amounts of actually grafted PLL, zeta potential values and N atomic weight fractions were measured for all the hydrogels after complete removal of the sol fraction. As shown in Figure 3a, the zeta potential at pH 7.4 gradually increased from 0.16 ± 0.07 mV for the neutral hydrogel to 14.3 ± 0.5 mV for the PLL-grafted hydrogels with ϕ_{PLL} of 5%. The amounts of PLL grafted in the networks were calculated from the weight fractions of N atoms in the total amounts of C, O, and N atoms in dried hydrogels, which were obtained from EDS measurements. The amount of actually grafted PLL in the networks increased proportionally with ϕ_{PLL}. The PLL graft ratios were 0.53, 0.50, 0.48, and 0.42 for the PLL-grafted hydrogels at ϕ_{PLL} of 1%, 2%, 3%, and 5%, respectively. Untethered PLL chains might be the result of lower reactivity of photo-polymerization for the allyllic double bond from PLL than the acrylate groups from PEGDA in dilute aqueous solutions. As shown in Figure 3b, the amounts of grafted PLL in the hydrogels were in a good linear relationship (slope = 2.17, intercept = 0.05, R = 0.9993) with their zeta potential values, indicating that the positive charge densities of the hydrogels were dependent on dissociated amine groups of pendent PLL chains. The coverage of PLL chains on the surface of PEGDA hydrogels was estimated using the Kuhn length b of 3.6 nm for PLL[27] and 0.7 nm for PEG[28] and the mean-square radius of gyration R_g^2 of them. R_g^2 for tethered PLL chains was calculated to be 97.4 nm^2 using eq. 1[29] and R_g^2 for PEGDA hydrogels in swollen state was calculated to be 54.6 nm^2 using eq. 2.[30]

$$R_{g,PLL}^2 = \frac{(N^{3/5}b)^2}{6} \quad (1)$$

$$R_{g,PEGDA}^2(swollen) = R_{g,PEGDA}^2(\theta)\varphi_{PEGDA}^{-1/8} = \frac{(N^{1/2}b)^2}{6}\varphi_{PEGDA}^{-1/8} \quad (2)$$

where N is the number of repeating units, $R_{g,PEGDA}^2(\theta)$ is the R_g^2 for PEGDA hydrogels in θ condition, and φ_{PEGDA} is the volume fraction of PEGDA hydrogel in water obtained from the swelling ratio. Calculated from the amounts of grafted PLL measured using EDS, the molar fractions of actually grafted PLL (Φ_{PLL}) in the hydrogels were 7.7%, 13.6%, 18.4%, and 24.9% for PLL-grafted hydrogels at ϕ_{PLL} of 1%, 2%, 3%, and 5%, respectively. Therefore, the approximate coverage (C) values of grafted PLL chains on the surface calculated using eq. 3 were 13%, 22%, 29%, and 37% for the PLL-grafted hydrogels with ϕ_{PLL} of 1%, 2%, 3%, and 5%, respectively.

$$C = \frac{R_{g,PLL}^2 \cdot \Phi_{PLL}}{R_{g,PLL}^2 \cdot \Phi_{PLL} + R_{g,PEGDA}^2(swollen) \cdot (1 - \Phi_{PLL})} \quad (3)$$

These results confirmed the positively charged nature of hydrogels and different amounts of covalently grafted PLL chains could result in different PLL coverage on the hydrogels, which consequently could influence NPC behavior as discussed in the following contents.

NPC Viability in Encapsulation

NPCs were photo-encapsulated and cultured in the hydrogels for 7 and 14 days to investigate the effect of PLL grafting density on the cell survival in 3D hydrogels. From the LIVE/DEAD assay that stained live cells green and dead cells red in Figure 4a, we counted the percentage of live cells in the entire cell population at these two time points, which was cell viability in Figure 4b. The NPC viability was 87% in the neutral hydrogel at day 7, and it increased to 92% and ~95% for the PLL-grafted hydrogels with ϕ_{PLL} of 1% and 2-5%, respectively. More red cells were seen after a longer period of 14 days in the neutral hydrogel and the cell viability significantly decreased to 79%; however, there was only a slight decrease to 88% and ~92% without statistically significant difference from the values at day 7 in the PLL-grafted hydrogels with ϕ_{PLL} of 1% and 2-5%, respectively. These results suggested that the pendent PLL chains with positive charges in the hydrogels could significantly improve the viability of NPCs. Previously we examined the viability of encapsulated PC12 cells in the PLL-grafted hydrogel with ϕ_{PLL} of 1% for no more than 7 days, showing consistent results of much higher PC12 viability than in the neutral hydrogel.[8] The present study also demonstrated the effect of PLL grafting density on NPC viability, higher ϕ_{PLL} of 2-5% could provide better support for cell survival than ϕ_{PLL} of 1%. These PLL-grafted hydrogels could serve as a good cell delivery vehicle to maintain high cell viability (> 90%) for as long as 14 days, similar to the effect of tethered RGD peptide or soluble factors such as collagen and bFGF, which could support cell survival in 3D matrices as well.[10-13]

NPC Attachment and Proliferation

The effect of PLL grafting density on the attachment and proliferation of NPCs was evaluated in serum-free conditions, where the factor of serum protein adsorption on the hydrogels could be excluded. As shown in the DAPI-stained fluorescence images in Figure 5a, the size and number of neurospheres on the hydrogels demonstrated their dependence on ϕ_{PLL}. The PLL-grafted hydrogels always supported more NPCs than the neutral hydrogels at all time points. Normalized NPC attachment (Figure 5b) was determined at 12 h post-seeding. Only ~70% NPCs attached on the neutral hydrogels relative to tissue-culture polystyrene (TCPS), which was the positive control set with 100% attachment. The NPC attachment gradually increased to ~87% and ~110% for PLL-grafted hydrogels with ϕ_{PLL} of 1% and 2-5%, respectively. We have found a similar trend for the effect of ϕ_{PLL} on NPC proliferation over 7 days (Figure 5c), where the cell number increased on the hydrogels grafted with more PLL chains up to ϕ_{PLL} of 3%. The proliferation index (PI), i.e., the ratio of the cell number at day 7 to the attached cell number at 12 h post-seeding, weakly varied from 5.0 ± 0.3 on the neutral hydrogel to 5.2 ± 0.4 and ~5.4 on the PLL-grafted hydrogels with ϕ_{PLL} of 1% and 2-5%, respectively. This result suggested that the difference in the cell numbers at longer time was mainly determined by the initial cell attachment. Consistent with our previous result that the PLL-grafted hydrogel at ϕ_{PLL} of 1% showed better NPC attachment and proliferation than the neutral hydrogel,[8] the present results demonstrated that an optimal PLL grafting density for promoting cell attachment and proliferation was at ϕ_{PLL} of 2-5%. As mentioned earlier, the free amine groups on the PLL chains produce a basic monopolar surface to facilitate cell adhesion through electrostatic interaction.[16] Enhancement of grafted PLL chains in NPC attachment was greater than that in PI because PLL chains could best interact with the negative charges on the cell membrane during cell attachment and early proliferation period, which occur within one day post-seeding, while newly proliferated cells can form larger cell aggregates or neurospheres, which are

prohibited from interacting with the substrates.[31] We have also immunostained NPCs after 7-day proliferation with nestin, a neural progenitor specific marker, to confirm the progenitor nature of cells prior to further studies of cell differentiation toward different lineages and their gene expression.[31,32] Almost 100% of cells remained nestin-positive on all the hydrogels, indicating that cells maintained an immature and undifferentiated state in the serum-free growth media.

NPC Differentiation

NPCs differentiated into all three primary CNS lineages of neurons, astrocytes, and oligodendrocytes on the PLL-grafted hydrogels in mixed differentiation media (1% FBS)[31,32] to investigate the effect of PLL grafting density on the lineage commitment. NPCs at a lower density of 5000 cells/cm^2 was seeded on the PLL-grafted hydrogels to ensure sufficient space for cell differentiation, neurite outgrowth, and interactions between cells and substrates rather than forming neurospheres with dominant cell-cell contact at high cell densities. Phase-contrast and fluorescence images immunostained using differentiation markers were assessed to determine the lineage commitment of NPCs and their morphological characteristics. As shown from the optical images in Figure 6, most cells remained a round phenotype and only a few cells extended short neurites on the neutral hydrogels, while many more cells bearing neurites were found on the PLL-grafted hydrogels with ϕ_{PLL} of 1-3%. NPCs differentiated on the hydrogels with a higher PLL density (ϕ_{PLL} = 5%) but did not form many neurites. NPCs stained with a mature neuronal marker NF displayed typical neurite morphology and best neurite extension on the PLL-grafted hydrogels with ϕ_{PLL} of 2%, whereas only a few mature neurites extended on the neutral hydrogels or hydrogels with ϕ_{PLL} of 5%. Double immunohistochemistry of β-tubulin III (green) and GFAP (red) demonstrated a comparison between neuronal and astrocytic differentiation, indicating that both lineages were promoted on the PLL-grafted hydrogels. Oligodendrocytes were also evaluated by staining differentiated NPCs with O4 marker. Not many cells expressed O4 and typical oligodendrocytes were not exhibited on all the hydrogels.

The percentage of differentiation toward each lineage was quantified by dividing the number of antibody-positive cells by the total cell number, as shown in Figure 7. The total percentage of NPC differentiation (Figure 7a) toward all three lineages increased dramatically from 31 ± 8% on the neutral hydrogels to 85 ± 11% at ϕ_{PLL} of 1% and 100 ± 15% at ϕ_{PLL} of 2%, while higher ϕ_{PLL} of 5% resulted in decreased differentiation of 61 ± 19%. A similar non-monotonic dependence on ϕ_{PLL} was found for neuronal differentiation (Figure 7b) as the highest percentage of ~44% NPCs expressed NF on the hydrogels with an intermediate PLL grafting density at ϕ_{PLL} of 2%, while higher ϕ_{PLL} of 5% less supported differentiation toward mature neurons. Astrocytic differentiation (Figure 7c) demonstrated a much higher percentage of ~40% for hydrogels at ϕ_{PLL} of 1-3%, while only ~8% and ~25% of astrocytes were differentiated on the neutral hydrogels and PLL-grafted hydrogels at ϕ_{PLL} of 5%, respectively. Oligodendrocyte differentiation (Figure 7d) was not well supported on all the hydrogels under the current differentiation condition. Only ~7% O4-positive cells were found on the neutral hydrogels and this percentage slightly increased to ~14% for all the PLL-grafted hydrogels.

Besides the percentage of differentiated NPCs that displayed neuronal morphology, we also quantified neurite formation on these cells from NF-immunostained images, as exhibited in Figure 8. Again, a parabolic or non-monotonic trend with ϕ_{PLL} was shown in the percentage of cells bearing neurites (Figure 8a) and the number of mature neurites per cell or neurite-bearing cell (Figure 8b) and the highest number was found on the hydrogels with ϕ_{PLL} of 2%. Neurite extension in terms of the average neurite length (Figure 8c) and the total neurite length per cell or neurite-bearing cell (Figure 8d) also showed the same trend. For example,

the average neurite length increased significantly from 16 ± 5 μm on neutral hydrogels to 27 ± 11 and 37 ± 14 μm on the hydrogels with ϕ_{PLL} of 1% and 2%, and then decreased to 22 ± 9 μm at higher ϕ_{PLL} of 5%. The distinct morphologies of single NPCs with typical neurite outgrowth on the hydrogels with different ϕ_{PLL} could be seen from the fluorescence images in Figure 8e.

NPC Gene Expression

Gene expression of differentiated NPCs for 7 days was conducted using real-time PCR to further understand their fate decisions on the hydrogels with different PLL grafting densities. As shown in Figure 9a, the nestin expression normalized to the level of housekeeping gene GAPDH was low (~0.017) on the neutral hydrogels and even lower (~0.004) on the PLL-grafted hydrogels with ϕ_{PLL} of 2%, in agreement with the immunostained images that much fewer immature NPCs appeared on the PLL-grafted hydrogels than on the neutral ones after 7-day differentiation. The low expression and down-regulation of nestin in differentiation can be seen in previous reports that the nestin mRNA level decreased by over 10 folds at day 8 compared with day 0.[31] The expression levels of β-tubulin III (Figure 9b), an early neuronal marker, and NSE (Figure 9c), a mature neuronal marker, both demonstrated a non-monotonic dependence on ϕ_{PLL} for differentiated NPCs. They first significantly increased from the neutral hydrogel to the PLL-grafted hydrogels with ϕ_{PLL} of 2%, and then decreased at higher ϕ_{PLL} of 3-5%. Much higher expression of NSE than β-tubulin III indicated that more mature neurons were differentiated on the hydrogels. A similar trend on ϕ_{PLL} was found for the expression of GFAP (Figure 9d), an astrocyte marker, which maximized on the PLL-grafted hydrogels with ϕ_{PLL} of 2%. As shown in Figure 9e, the mature oligodendrocyte marker MOG yielded relatively low expression (< 0.15) for all the samples compared with other lineages. It was consistent with fewer O4-positive cells than other markers quantified from fluorescence images, but a similar trend could still be seen as that expression on the hydrogels with ϕ_{PLL} of 2-3% was upregulated compared with other compositions.

Further Discussion

Chemical, topological and mechanical properties are three major determining factors for biomaterials to influence cell functions.[33] In this study, the surface chemistry of PEGDA hydrogels was modified by different amounts of tethered PLL chains. Because of the dissociation of the primary amine groups, PLL grafted on the hydrogels can introduce positive charges and monopolar basic surface to modulate NPC adhesion and other adhesion-mediated cell behaviors via electrostatic interaction with the negatively charged cell membrane.[16,34-37] Despite the degradability of PEGDA-based hydrogels, in the duration for our studies, i.e., 7 and 14 days, no evident degradation or decrease in mechanical properties was found.

The effect of PLL on cell behavior depends on the amount of amine groups, which is determined by both the molecular weight and concentration.[19,34-37] Our PLL-grafted PEGDA hydrogels all could promote NPC viability in 3D encapsulation, attachment and proliferation with dependence on the PLL grafting density up to ϕ_{PLL} of 2%. Meanwhile, no cytotoxic effect of PLL was observed at ϕ_{PLL} of 1-5% when NPCs were encapsulated in the hydrogels. The reasons might be the low molecular weight PLL (~3000 g/mol) and the extensive swelling of the hydrogels. For NPC differentiation, however, we observed a parabolic or non-monotonic trend, showing that an optimal ϕ_{PLL} of 2% could best promote both neuronal and astrocytic differentiation. Grafted PLL on the hydrogels were also found to influence cellular differentiation pathways that upregulated mRNA gene expression of both mature neuronal and astrocytic markers at an intermediate grafting density when ϕ_{PLL} was 2%. The difference in 2D and 3D cell culture can be a simple reason for the distinct

dependence on ϕ_{PLL} between viability and differentiation,[38] as the mesh size in the hydrogels and permeability increased with incorporating more PLL and thus the environment for photo-encapsulated NPCs was improved. The promoted NPC differentiation into both neuronal and glial lineages and extensive neurite outgrowth on the hydrogel with an optimal PLL density is critical for its application in guiding neurogenesis *in vivo* for nerve regeneration.[4] The mechanisms of fewer neurons and astrocytes and lower gene expression after differentiation at ϕ_{PLL} of 5% are not fully understood and warrant further investigation. The reasons might be that either these differentiated phenotypes could not survive or the downstream cellular pathways were altered by densely grafted PLL chains.

A previous study found that 5 μg/mL PLL (400000 g/mol) coated on glass surface promoted attachment of embryonic brain cells.[16] In another study, a lower concentration (1 μg/mL) of PLL (70000-150000 g/mol) could enhance MSC adhesion, spreading, proliferation, and chondrogenic differentiation, while a higher concentration of PLL (10 μg/mL) induced cell detachment and spheroid formation.[34] An optimal concentration (0.5%) of poly(D-lysine) (1000-4000 g/mol) was reported to improve the 2D neuronal survival and neurite extension when immobilized onto chitosan, while a higher concentration decreased the cell number and neurite lengths.[35] Spreading of red blood cells was studied on glass slides coated with PLL of different molecular weights and concentrations.[36] The largest cell spreading was observed on glass treated by PLL coating solutions with molecular weights and concentrations of 500 g/mol and 100 mg/mL, 3800 g/mol and 10 mg/mL, or 72000 g/mol and 0.1 mg/mL.[36] Low PLL concentrations were found to only weakly enhance cell adhesion, whereas high concentrations and molecular weights induced cell lysis.[36] The viability of L929 mouse fibroblast was found to decrease in PLL solutions (36600 g/mol, 0.1 mg/mL), showing the toxic effect of PLL solutions at high concentrations, which might be because of too strong interactions of polycations with cell membranes or their influence on intracellular signal transduction pathways.[37] These previous results demonstrated that PLL chains are beneficial for cell functions in a concentration or surface density range that varies for different cell types and substrates, consistent with our findings on NPCs.

A similar concentration dependence for cell responses has been seen in other polycations such as poly(ethylenimine) and small-molecular MTAC.[14,15,37] The effect of PLL on enhancing NPC behavior was previously demonstrated by us to be better than MTAC at the same or even lower charge density, suggesting that PLL was more cytocompatible.[8] Despite a non-receptor-mediated mechanism, the promotional effect of PLL on cell functions found in this study can be similar to RGD-modified PEGDA hydrogels,[11-13] although further studies are needed to provide direct evidence. The concentration dependence of the cell adhesive molecules such as RGD, laminin, or collagen was found to be different from PLL because these molecules mediate cell adhesion via integrin receptors and they only show promotion for cell adhesion until saturation effect occurs at a high concentration.[11-13,39]

Besides the effect of PLL on cell functions in this study, the factor of mechanical properties could also be involved to modulate NPC behavior for hydrogels at higher ϕ_{PLL} of 3-5%, whereas the factor of surface topography could be neglected because the high gel fractions of all the hydrogels ensured similar smooth surfaces. The rheological data in Figure 2b indicated that the PLL-grafted hydrogels with ϕ_{PLL} of 1-2% were similar to the neutral hydrogels at G of ~9 kPa, which can be converted to elastic modulus (E) of ~27 kPa using the equation of $E = 3G$.[20,40] Decreased E was found to be ~20 and ~14 kPa for the PLL-grafted hydrogels at higher ϕ_{PLL} of 3% and 5%, respectively. A lower E range of 0.5-750 kPa for hydrogels was previously found to promote cell survival, attachment, proliferation, and differentiation toward neurons while inhibiting astroctyes for neural stem/progenitor cells.[8,31,40] Therefore, the similar cell viability, attachment, and proliferation, as well as less

astrocytes for PLL-grafted hydrogels at higher ϕ_{PLL} of 3-5% compared with ϕ_{PLL} of 2% might be attributed partially to their lower moduli, as well as the higher mesh size and permeability discussed earlier. For differentiation toward neurons, PLL effect was so dominant that percentage of neurons did not increase at high ϕ_{PLL}. Further studies are still required to differentiate the effect of PLL and stiffness at high ϕ_{PLL} in regulating NPC behavior.

Designing a bioactive cell carrier is of pivotal importance for the use of NPCs in nerve repair and regeneration.[4-6] Numerous studies have been conducted to explore the potential of PEG-based hydrogels to deliver NPCs for neural transplantation.[7,8,10,18,19] NPCs encapsulated in pristine PEG hydrogels were able to survive and maintain their ability to proliferate and differentiate, consistent with our results.[10] Both the mesh size and chemistry of PEG hydrogels were critical for creating a better NPC niche and thus various strategies have been used to incorporate bioactive molecules into the hydrogels.[7,8] For example, the effect of soluble factors such as collagen and bFGF were investigated to improve the chemical microenvironment for NPCs.[10] On the basis of linkage to the free amine groups, Hynes *et al.* developed PLL-*g*-PEG hydrogels to encapsulate NPCs and they found that 55% cells differentiated into neuronal cell type while few cells expressed astrocytic markers and 44% cells remain undifferentiated after 17-day culture in differentiation media containing epidermal growth factor.[19]

Although PLL has long been used in the standard coating technique on petri dishes to enhance cell adhesion, the method of covalently linking PLL to the polymer networks without functioning amine groups is rare. The present study suggests an efficient method to incorporate PLL chains at various ϕ_{PLL} into the PEGDA hydrogel. Moreover, covalent tethering of PLL chains on the PEGDA hydrogels ensured long-term effectiveness both on the surface and inside the hydrogels even after biodegradation. Because of the dissociation of primary amine groups, the amount of PLL chains could be easily characterized by zeta potentials and N content, showing a proportional increase with ϕ_{PLL} and a fairly constant grafting efficiency of ~50%, and facilitating further cell studies on the effect of PLL grafting density. These free amine groups in PLL open a door to further chemical incorporation of specific cell adhesion peptides.[19,41] The PLL-grafted hydrogels with an optimal ϕ_{PLL} of 2% demonstrated the ability to best promote NPC viability in encapsulation, attachment, proliferation, differentiation toward all three lineages, and neurite outgrowth, which may lead to better neurogenesis *in vivo*.[4] In future, we will explore the applications of this hydrogel with NPCs *in vitro* and *in vivo* for treatment of nerve injuries.

Conclusions

We have prepared a series of PLL-grafted hydrogels by photo-crosslinking polymerizable PLL with PEGDA at various ϕ_{PLL} of 0-5% in DI water. The PLL grafting densities and the charge densities of the hydrogels were characterized and proportionally correlated with the feed compositions. The viability of mouse NPCs in 3D encapsulation in the hydrogels and their attachment and proliferation on the hydrogel disks were significantly promoted compared with the neutral ones up to ϕ_{PLL} of 2%. NPC differentiation into different lineages demonstrated a parabolic or non-monotonic dependence on ϕ_{PLL}. Significant increases in mature neurons and extensive neurite outgrowths as well as in astrocytes were found on the PLL-grafted hydrogels with ϕ_{PLL} up to 2%, whereas fewer differentiated NPCs were shown at higher ϕ_{PLL} of 5%. Gene expression of differentiated NPCs further elicited the promoted mRNA expression of lineage markers on hydrogels with intermediate PLL grafting densities. The present results demonstrated that the PLL-grafted hydrogels with an optimal ϕ_{PLL} of 2% had great potential as a cell carrier and luminal filler in nerve guides for fostering nerve repair and regeneration.

Acknowledgments

This work was supported by the start-up fund and professional development award from the University of Tennessee, and in part, by National Science Foundation (DMR-11-06142, to S.W.). We thank Minfeng Jin and Dr. Federico M. Harte for assistance with zeta-potential measurements.

References

1. Schmidt CE, Leach JB. Annu Rev Biomed Eng. 2003; 5:293. [PubMed: 14527315]
2. Chiono V, Tonda-Turo C, Ciardelli G. Int Rev Neurobiol. 2009; 87:173. [PubMed: 19682638]
3. Madigan NN, McMahon S, O'Brien T, Yaszemski MJ, Windebank AJ. Respir Physiol Neurobiol. 2009; 169:183. [PubMed: 19737633]
4. (a) Gage FH. Science. 2000; 287:1433. [PubMed: 10688783] (b) Temple S. Nature. 2001; 414:112. [PubMed: 11689956] (c) Cummings BJ, Uchida N, Tamaki SJ, Salazar DL, Hooshmand M, Summers R, Gage FH, Anderson AJ. Proc Natl Acad Sci USA. 2005; 102:14069. [PubMed: 16172374] (d) Teng YD, Lavik EB, Qu X, Park KI, Ourednik J, Zurakowski D, Langer R, Snyder EY. Proc Natl Acad Sci USA. 2002; 99:3024. [PubMed: 11867737]
5. Wang S, Cai L. Biomaterials. 1054Kulshrestha, AS.; Mahapatro, A.; Henderson, LA. American Chemical Society. Vol. Ch 3. Washington, DC: 2010.
6. Wang S, Cai L. Int J Polym Sci. 2010:138686.
7. Zhu J. Biomaterials. 2010; 31:4639. [PubMed: 20303169]
8. Cai L, Lu J, Sheen V, Wang S. Biomacromolecules. 2012; 13:342. [PubMed: 22251248]
9. Cai L, Wang S. Biomacromolecules. 2010; 11:304. [PubMed: 20000349]
10. (a) Mahoney MJ, Anseth KS. J Biomed Mater Res. 2007; 81A:269.(b) Mahoney MJ, Anseth KS. Biomaterials. 2006; 27:2265. [PubMed: 16318872]
11. Burdick JA, Anseth KS. Biomaterials. 2002; 23:4315. [PubMed: 12219821]
12. Petrie TA, Capadona JR, Reyes CD, Garcia AJ. Biomaterials. 2006; 27:5459. [PubMed: 16846640]
13. Yang F, Williams CG, Wang D-A, Lee H, Manson PN, Elisseeff J. Biomaterials. 2005; 26:5991. [PubMed: 15878198]
14. Dadsetan M, Knight AM, Lu L, Windebank AJ, Yaszemski MJ. Biomaterials. 2009; 30:3874. [PubMed: 19427689]
15. Sosnik A, Sefton MV. J Biomed Mater Res. 2005; 75A:295.
16. (a) Rao SS, Winter JO. Front Neuroeng. 2009; 2:1. [PubMed: 19194527] (b) Yavin E, Yavin Z. J Cell Biol. 1974; 62:540. [PubMed: 4609989]
17. Khademhosseini A, Suh KY, Yang JM, Eng G, Yeh J, Levenberg S, Langer R. Biomaterials. 2004; 25:3583. [PubMed: 15020132]
18. Rao SS, Han N, Winter JO. J Biomater Sci Polym Ed. 2011; 22:611. [PubMed: 20566048]
19. (a) Hynes SR, McGregor LM, Rauch MF, Lavik EB. J Biomater Sci Polym Ed. 2007; 18:1017. [PubMed: 17705996] (b) Hynes SR, Rauch MF, Bertram JP, Lavik EB. J Biomed Mater Res Part A. 2009; 89:499.
20. Wang S, Kempen DH, Simha NK, Lewis JL, Windebank AJ, Yaszemski MJ, Lu L. Biomacromolecules. 2008; 9:1229. [PubMed: 18307311]
21. Wang S, Yaszemski MJ, Knight AM, Gruetzmacher JA, Windebank AJ, Lu L. Acta Biomater. 2009; 5:1531. [PubMed: 19171506]
22. Cai L, Wang S. Polymer. 2010; 51:164.
23. Cai L, Wang S. Biomaterials. 2010; 31:7423. [PubMed: 20663551]
24. Chen YM, Ogawa R, Kakugo A, Osada Y, Gong JP. Soft Matter. 2009; 5:1804.
25. Cai L, Wang K, Wang S. Biomaterials. 2010; 31:4457. [PubMed: 20202682]
26. Cai L, Lu J, Sheen V, Wang S. Biomacromolecules. 2012; 13:358. [PubMed: 22206477]
27. Maurstad G, Danielsen S, Stokke BT. J Phys Chem B. 2003; 107:8172.
28. Schultz KM, Baldwin AD, Kiick KL, Furst EM. Macromolecules. 2009; 42:5310. [PubMed: 21494422]

29. (a) Halperin A, Tirrell M, Lodge TP. Adv Polym Sci. 1992; 100:31.(b) Zhao B, Brittain WJ. Prog Polym Sci. 2000; 25:677.
30. Horkay F, Stanley HB, Geissler E, King SM. Macromolecules. 1995; 28:678.
31. Leipzig ND, Shoichet MS. Biomaterials. 2009; 30:6867. [PubMed: 19775749]
32. (a) Ray J, Gage FH. Mol Cell Neurosci. 2006; 31:560. [PubMed: 16426857] (b) Aizawa Y, Leipzig ND, Zahir T, Shoichet MS. Biomaterials. 2008; 29:4676. [PubMed: 18801569]
33. (a) Saltzman, WM.; Kyriakides, TR. Principles of tissue engineering. 3. Lanza, R.; Langer, R.; Vacanti, J., editors. Elsevier Academic Press; San Diego, CA: 2007. p. 279-296.(b) Harbers, GM.; Grainger, DW. Introduction to biomaterials. Guelcher, SA.; Hollinger, JO., editors. CRC Press; Boca Raton, FL: 2005. p. 15-45.
34. Lu H, Guo L, Kawazoe N, Tateishi T, Chen G. J Biomater Sci. 2009; 20:577.
35. Crompton KE, Goud JD, Bellamkonda RV, Gengenbach TR, Finkelstein DI, Horne MK, Forsythe JS. Biomaterials. 2007; 28:441. [PubMed: 16978692]
36. Hategan A, Sengupta K, Kahn S, Sackmann E, Discher DE. Biophys J. 2004; 87:3547. [PubMed: 15339814]
37. Fischer D, Li Y, Ahlemeyer B, Krieglstein J, Kissel T. Biomaterials. 2003; 24:1121. [PubMed: 12527253]
38. Lampe KJ, Mooney RG, Bjugstad KB, Mahoney MJ. J Biomed Mater Res. 2010; 94:1162.
39. Hersel U, Dahmen C, Kessler H. Biomaterials. 2003; 24:4385. [PubMed: 12922151]
40. Saha K, Keung AJ, Irwin EF, Li Y, Little L, Schaffer DV, Healy KE. Biophys J. 2008; 95:4426. [PubMed: 18658232]
41. Cook AD, Krkach JS, Gao NN, Johnson IM, Pajvani UB, Cannizzaro SM, Langer R. J Biomed Mater Res. 1997; 35:513. [PubMed: 9189829]

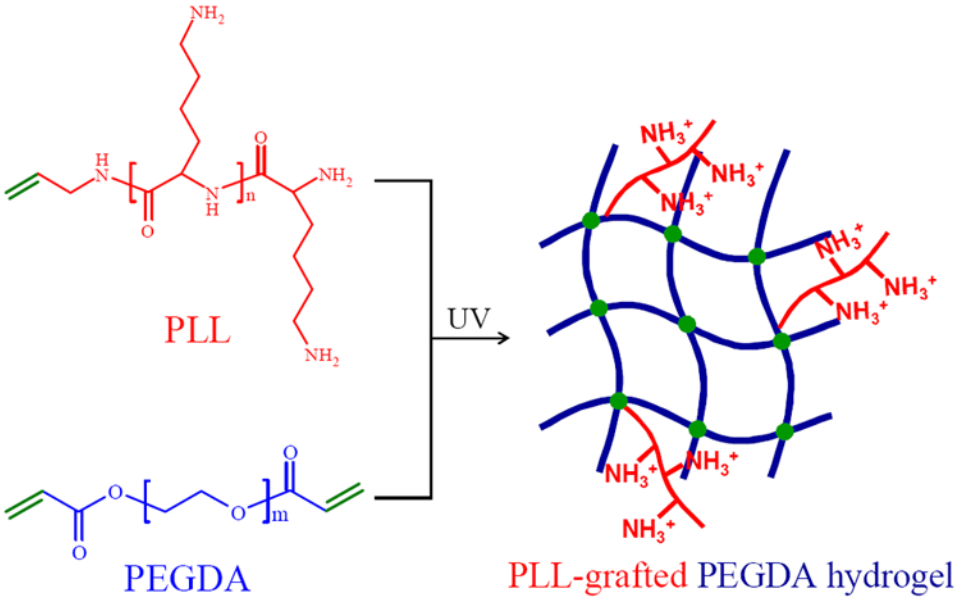

Figure 1.
Preparation of PLL-grafted PEGDA networks via photo-crosslinking. Integers *n* and *m* are estimated from M_n to be 23 and 327, respectively.

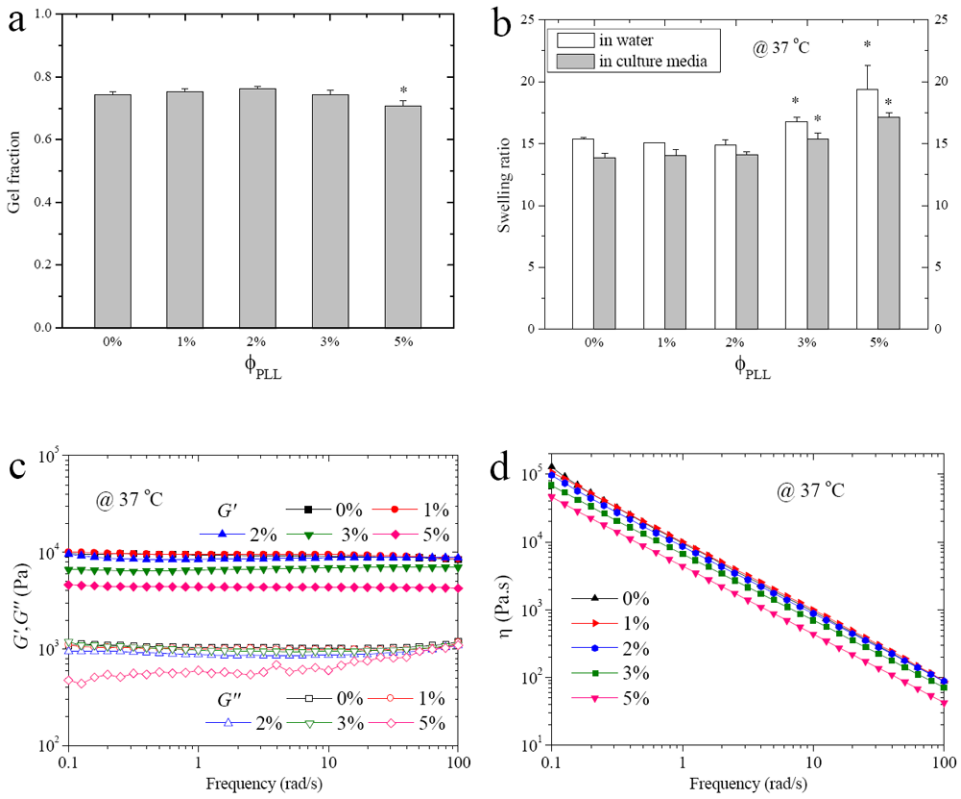

Figure 2.

(a) Gel fraction, (b) swelling ratios in DI water and culture media, (b) storage modulus *G'* and loss modulus *G"*, and (d) viscosity η at 37 °C vs. frequency for the neutral and PLL-grafted PEGDA hydrogels. *, $p < 0.05$ relative to other hydrogels.

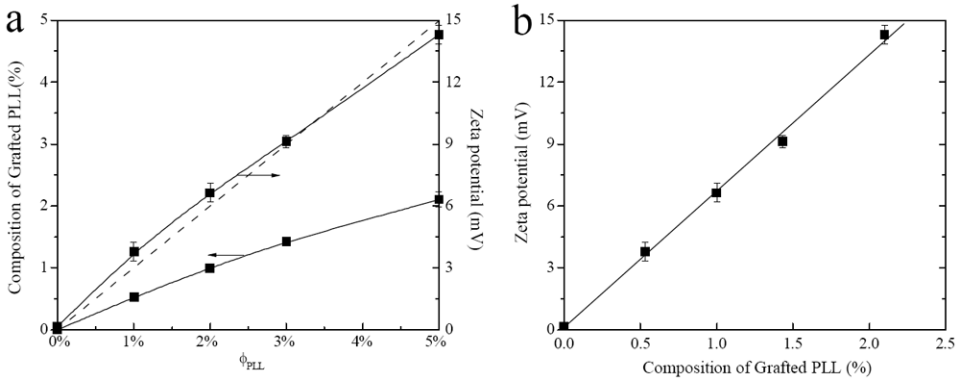

Figure 3.

(a) Composition of grafted PLL and zeta potential vs. feed composition of PLL (ϕ_{PLL}) for the neutral and PLL-grafted PEGDA hydrogels. The dashed diagonal line indicates the theoretical values if PLL grafting ratio is 100%. (b) Zeta potentials vs. composition of grafted PLL calculated from N atomic percentage. $p < 0.05$ between any two hydrogels.

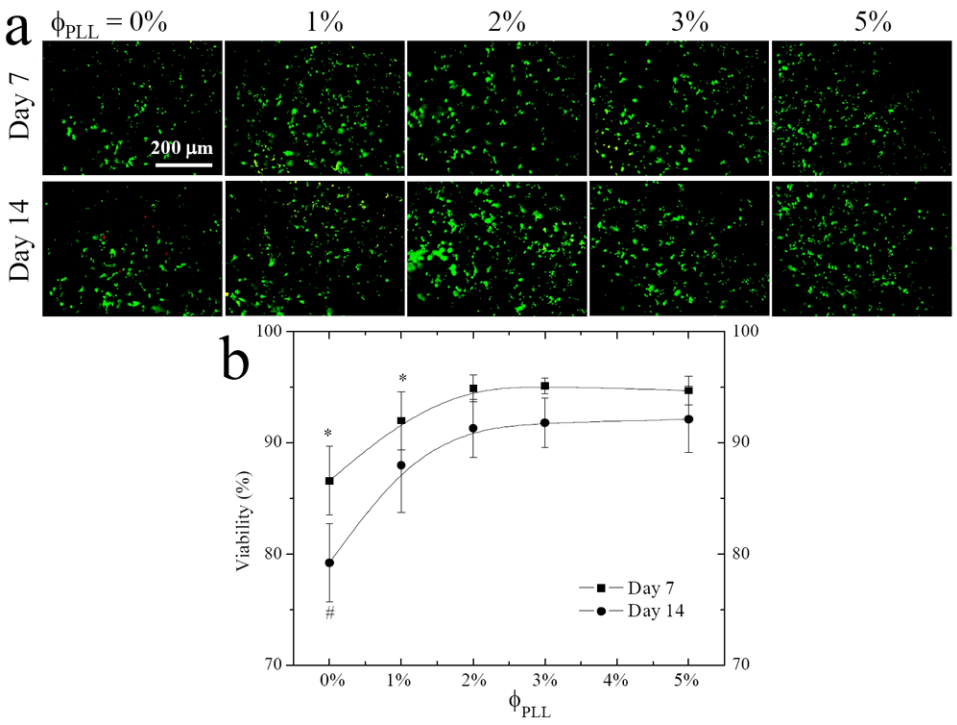

Figure 4.

NPC encapsulation in the neutral and PLL-grafted PEGDA hydrogels for 7 and 14 days. (a) Fluorescence images stained using LIVE-DEAD assay. Scale bar of 200 μm is applicable to all. (b) Cell viability after encapsulation. *, $p < 0.05$ relative to other hydrogels at day 7. #, $p < 0.05$ relative to other hydrogels at day 14 and hydrogel with ϕ_{PLL} of 0% at day 7.

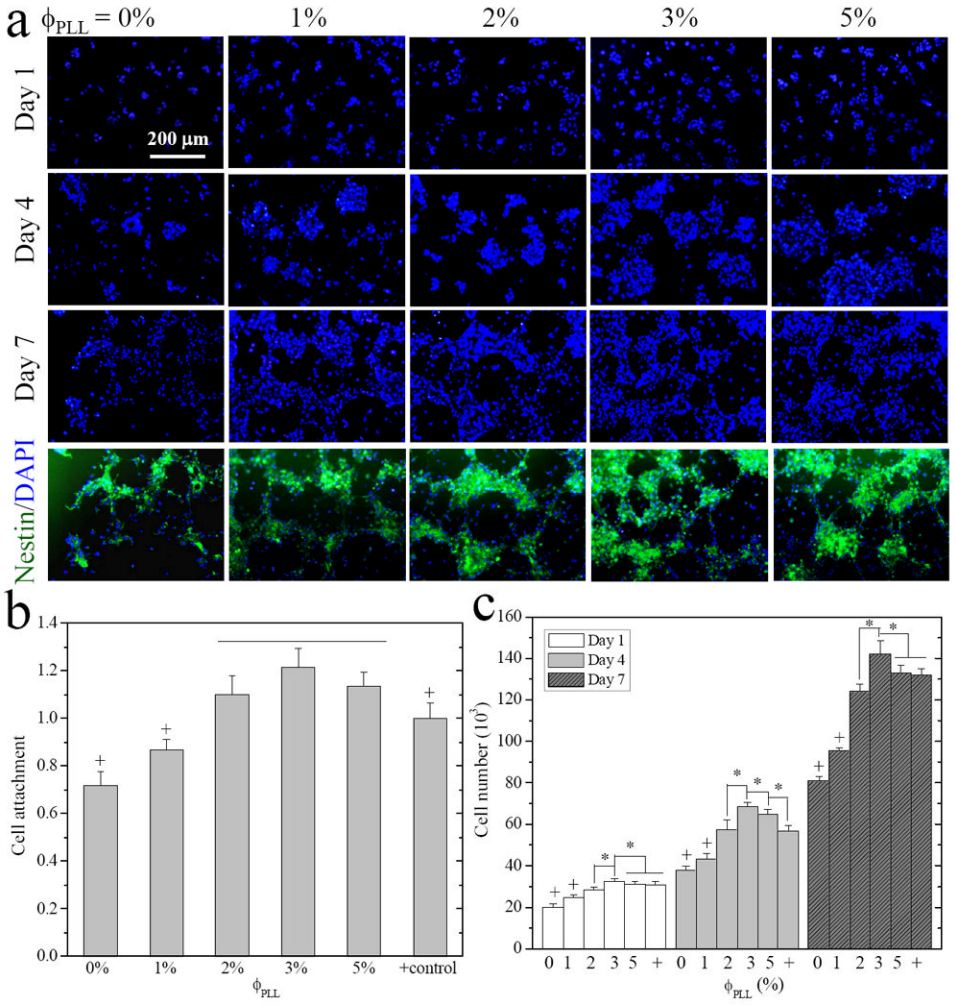

Figure 5.

E14 mouse NPC attachment and proliferation on the neutral and PLL-grafted PEGDA hydrogels. (a) Fluorescence images of neurospheres stained with DAPI (blue) at days 1, 4, and 7, and immunostained with anti-nestin (green, undifferentiated NPCs) in the same field at day 7 post-seeding. Scale bar of 200 μm is applicable to all. (b) Cell attachment at 12 h, and (c) cell numbers at days 1, 4, and 7, compared with cell-seeded TCPS as positive (+) control. *, $p < 0.05$. +, $p < 0.05$ relative to other hydrogels.

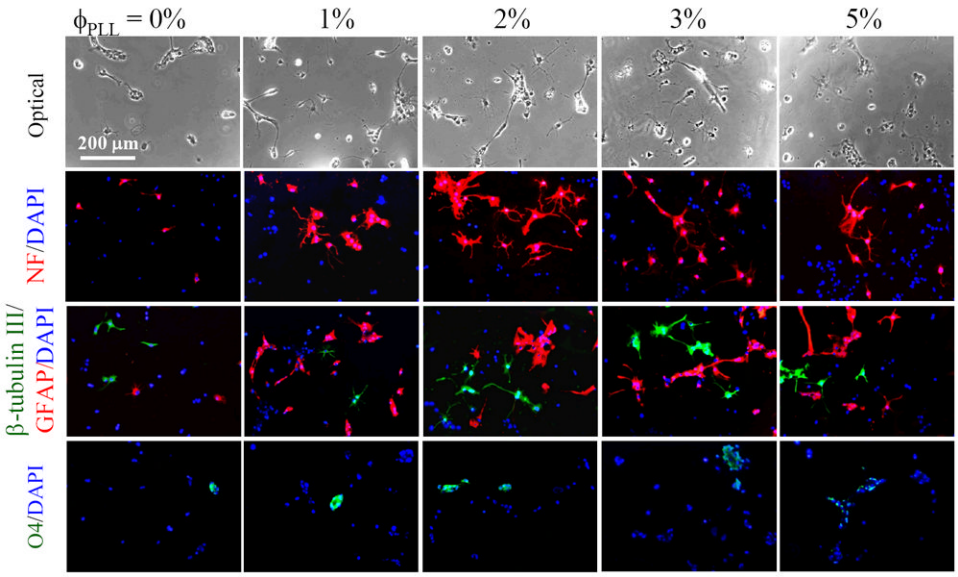

Figure 6.
Phase-contrast and fluorescence images of NPCs differentiated on the neutral and PLL-grafted PEGDA hydrogels for 7 days. Differentiated NPCs were immunostained with anti-NF (red, mature neurons), anti-β-tubulin III (green, immature neurons), anti-GFAP (red, astrocytes), and anti-O4 (green, oligodendrocytes), and counter-stained with DAPI (blue). Scale bar of 200 μm is applicable to all.

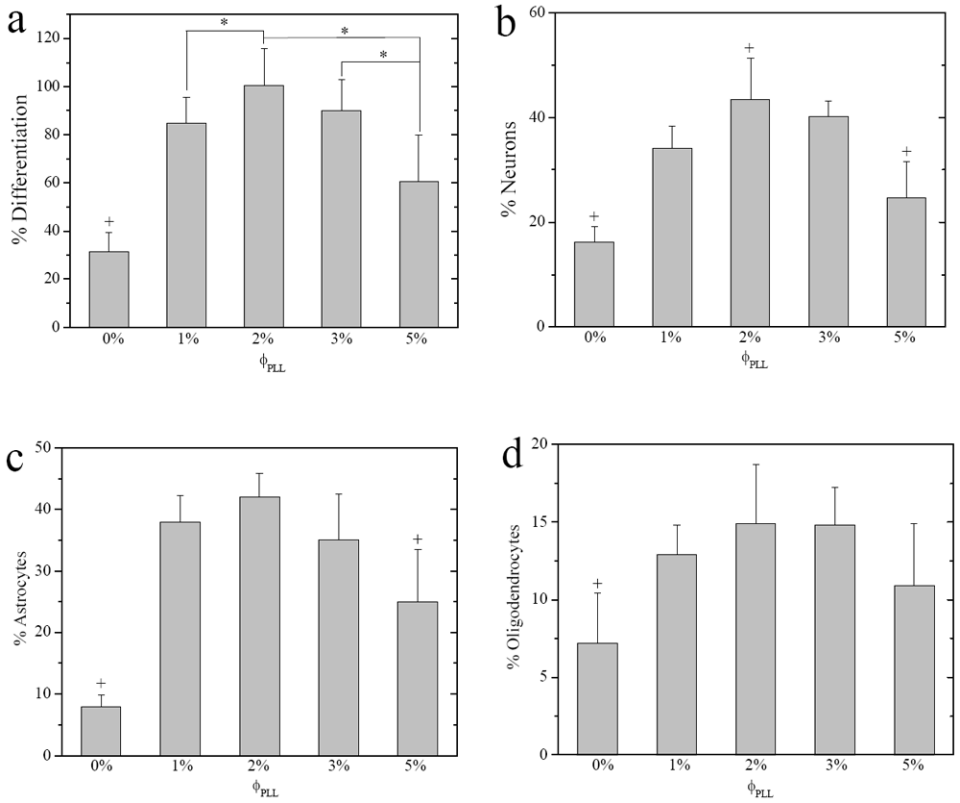

Figure 7.

Percentages of differentiated (a) NPCs, (b) neurons (NF-positive), (c) astrocytes (GFAP-positive), and (d) oligodendrocytes (O4-positive) on the neutral and PLL-grafted PEGDA hydrogels after 7-day culture in differentiation media. *, $p < 0.05$. +, $p < 0.05$ relative to other hydrogels.

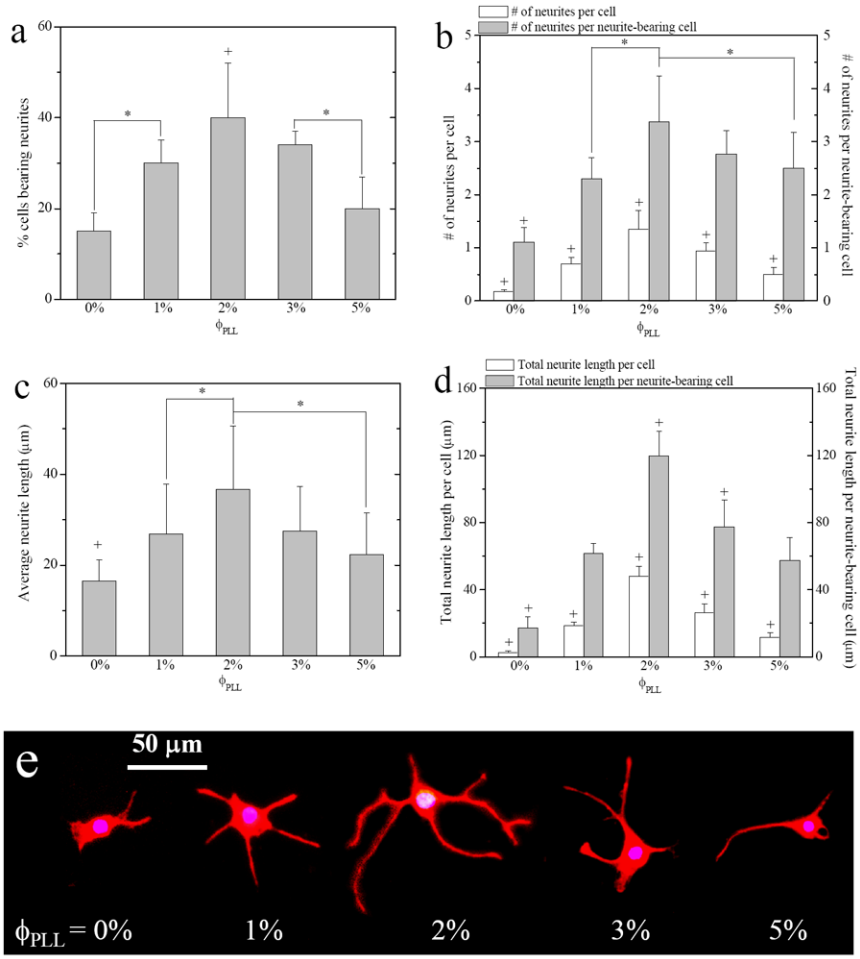

Figure 8.

(a) Percentage of neurite-bearing cells, (b) number of neurites per cell or per neurite-bearing cell, (c) average neurite length, (d) total neurite length per cell or per neurite-bearing cell, and (e) fluorescence images of NPC neurite outgrowth immunostained with NF on the neutral and PLL-grafted PEGDA hydrogels after 7-day culture in differentiation media. *, $p < 0.05$. +, $p < 0.05$ relative to other hydrogels.

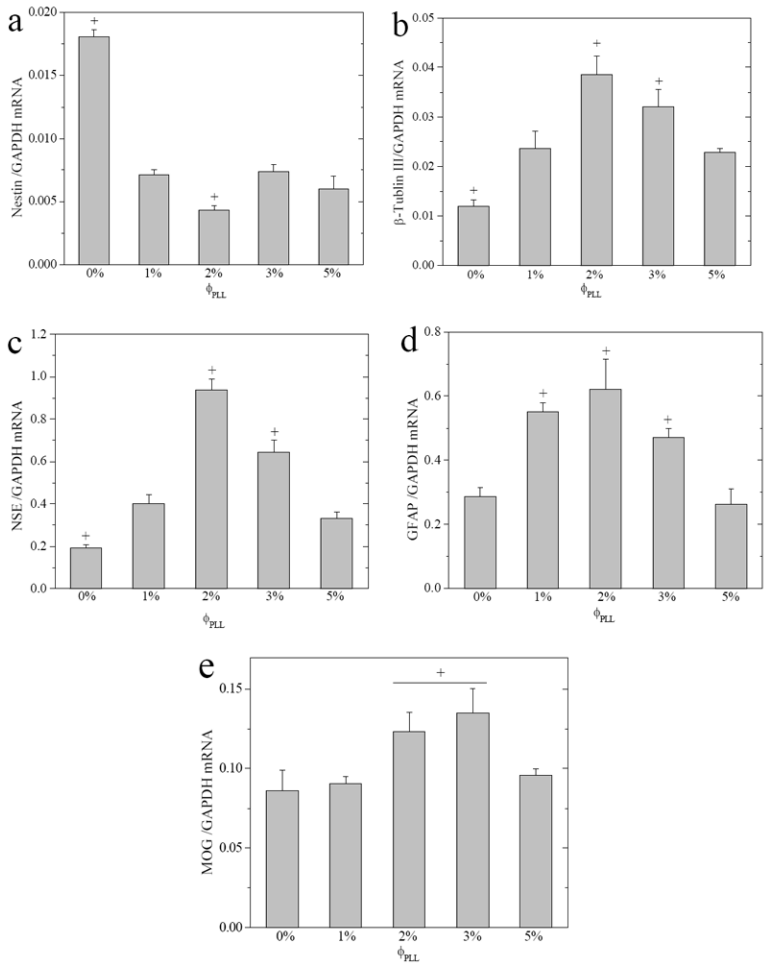

Figure 9.

Gene expression levels of (a) nestin, (b) β-tubulin III, (c) NSE, (d) GFAP, and (e) MOG, normalized to that of GAPDH for NPCs cultured on neutral and PLL-grafted PEGDA hydrogels in differentiation media for 7 days. +, $p < 0.05$ relative to other hydrogels.

Table 1

Oligonucleotide primer sequences for real-time PCR.

Primer	Accession #	Sequence (5' - 3')	Template	Product size (bp)
Nestin	NM_016701	CAA GAA CCA CTG GGG TCT GT	3396-3415	119
		CCT CCT GGT GAT TCC ACA GT	3495-3514	
β-tubulin III	NM_023279	CGA GAC CTA CTG CAT CGA CA	633-652	152
		CAT TGA GCT GAC CAG GGA AT	765-784	
NSE	NM_013509	TGA TCT TGT CGT CGG ACT GTG T	1234-1255	73
		CTT CGC CAG ACG TTC AGA TCT	1286-1306	
GFAP	X_02801	TGT GGA GGG TCC TGT GTG TA	7435-7454	199
		GTA GCC TGC TCC ACC TTC TG	7614-7633	
MOG	NM_010814	AAA TGG CAA GGA CCA AGA TG	240-259	140
		AGC AGG TGT AGC CTC CTT CA	360-379	
GAPDH	NM_008084	ACT TTG TCA AGC TCA TTT CC	961-980	267
		TGC AGC GAA CTT TAT TGA TG	1208-1227	